



The Inclusive Jet Cross Section in $p\bar{p}$ Collisions at $\sqrt{s} = 1.8$ TeV using the k_{\perp} Algorithm

The DØ Collaboration *

Fermi National Accelerator Laboratory, Batavia, Illinois 60510

(June 11, 2001)

Abstract

We present a preliminary measurement of the central inclusive jet cross section using a successive combination algorithm based on relative transverse momenta (k_{\perp}) for jet reconstruction. We analyze a 87.3 pb^{-1} data sample collected by the DØ detector at the Fermilab Tevatron $p\bar{p}$ Collider during 1994-1995. The cross section, reported as a function of transverse momentum ($p_T > 60$ GeV) in the central region of pseudo-rapidity ($|\eta| < 0.5$), is in reasonable agreement with next-to-leading order QCD predictions. This is the first jet production measurement in a hadron collider using a successive combination type of jet algorithm.

arXiv:hep-ex/0106032 v1 6 Jun 2001

*Submitted to the *International Europhysics Conference on High Energy Physics*, July 12-18, 2001, Budapest, Hungary,
and *XX International Symposium on Lepton and Photon Interactions at High Energies* July 23 – 28, 2001, Rome, Italy.

V.M. Abazov,²³ B. Abbott,⁵⁸ A. Abdesselam,¹¹ M. Abolins,⁵¹ V. Abramov,²⁶ B.S. Acharya,¹⁷
 D.L. Adams,⁶⁰ M. Adams,³⁸ S.N. Ahmed,²¹ G.D. Alexeev,²³ G.A. Alves,² N. Amos,⁵⁰
 E.W. Anderson,⁴³ Y. Arnoud,⁹ M.M. Baarmand,⁵⁵ V.V. Babintsev,²⁶ L. Babukhadia,⁵⁵
 T.C. Bacon,²⁸ A. Baden,⁴⁷ B. Baldin,³⁷ P.W. Balm,²⁰ S. Banerjee,¹⁷ E. Barberis,³⁰ P. Baringer,⁴⁴
 J. Barreto,² J.F. Bartlett,³⁷ U. Bassler,¹² D. Bauer,²⁸ A. Bean,⁴⁴ M. Begel,⁵⁴ A. Belyaev,³⁵
 S.B. Beri,¹⁵ G. Bernardi,¹² I. Bertram,²⁷ A. Besson,⁹ R. Beuselinck,²⁸ V.A. Bezzubov,²⁶
 P.C. Bhat,³⁷ V. Bhatnagar,¹¹ M. Bhattacharjee,⁵⁵ G. Blazey,³⁹ S. Blessing,³⁵ A. Boehnlein,³⁷
 N.I. Bojko,²⁶ F. Borchering,³⁷ K. Bos,²⁰ A. Brandt,⁶⁰ R. Breedon,³¹ G. Briskin,⁵⁹ R. Brock,⁵¹
 G. Brooijmans,³⁷ A. Bross,³⁷ D. Buchholz,⁴⁰ M. Buehler,³⁸ V. Buescher,¹⁴ V.S. Burtovoi,²⁶
 J.M. Butler,⁴⁸ F. Canelli,⁵⁴ W. Carvalho,³ D. Casey,⁵¹ Z. Casilum,⁵⁵ H. Castilla-Valdez,¹⁹
 D. Chakraborty,³⁹ K.M. Chan,⁵⁴ S.V. Chekulaev,²⁶ D.K. Cho,⁵⁴ S. Choi,³⁴ S. Chopra,⁵⁶
 J.H. Christenson,³⁷ M. Chung,³⁸ D. Claes,⁵² A.R. Clark,³⁰ J. Cochran,³⁴ L. Coney,⁴²
 B. Connolly,³⁵ W.E. Cooper,³⁷ D. Coppage,⁴⁴ S. Crépé-Renaudin,⁹ M.A.C. Cummings,³⁹
 D. Cutts,⁵⁹ G.A. Davis,⁵⁴ K. Davis,²⁹ K. De,⁶⁰ S.J. de Jong,²¹ K. Del Signore,⁵⁰ M. Demarteau,³⁷
 R. Demina,⁴⁵ P. Demine,⁹ D. Denisov,³⁷ S.P. Denisov,²⁶ S. Desai,⁵⁵ H.T. Diehl,³⁷ M. Diesburg,³⁷
 G. Di Loreto,⁵¹ S. Doulas,⁴⁹ P. Draper,⁶⁰ Y. Ducros,¹³ L.V. Dudko,²⁵ S. Duensing,²¹ L. Duflot,¹¹
 S.R. Dugad,¹⁷ A. Duperrin,¹⁰ A. Dyshkant,³⁹ D. Edmunds,⁵¹ J. Ellison,³⁴ V.D. Elvira,³⁷
 R. Engelmann,⁵⁵ S. Eno,⁴⁷ G. Eppley,⁶² P. Ermolov,²⁵ O.V. Eroshin,²⁶ J. Estrada,⁵⁴ H. Evans,⁵³
 V.N. Evdokimov,²⁶ T. Fahland,³³ S. Feher,³⁷ D. Fein,²⁹ T. Ferbel,⁵⁴ F. Filthaut,²¹ H.E. Fisk,³⁷
 Y. Fisyak,⁵⁶ E. Flattum,³⁷ F. Fleuret,³⁰ M. Fortner,³⁹ H. Fox,⁴⁰ K.C. Frame,⁵¹ S. Fu,⁵³
 S. Fuess,³⁷ E. Gallas,³⁷ A.N. Galyaev,²⁶ M. Gao,⁵³ V. Gavrilov,²⁴ R.J. Genik II,²⁷ K. Genser,³⁷
 C.E. Gerber,³⁸ Y. Gershtein,⁵⁹ R. Gilmartin,³⁵ G. Ginther,⁵⁴ B. Gómez,⁵ G. Gómez,⁴⁷
 P.I. Goncharov,²⁶ J.L. González Solís,¹⁹ H. Gordon,⁵⁶ L.T. Goss,⁶¹ K. Gounder,³⁷ A. Goussiou,²⁸
 N. Graf,⁵⁶ G. Graham,⁴⁷ P.D. Grannis,⁵⁵ J.A. Green,⁴³ H. Greenlee,³⁷ S. Grinstein,¹ L. Groer,⁵³
 S. Grünendahl,³⁷ A. Gupta,¹⁷ S.N. Gurzhiev,²⁶ G. Gutierrez,³⁷ P. Gutierrez,⁵⁸ N.J. Hadley,⁴⁷
 H. Haggerty,³⁷ S. Hagopian,³⁵ V. Hagopian,³⁵ R.E. Hall,³² P. Hanlet,⁴⁹ S. Hansen,³⁷
 J.M. Hauptman,⁴³ C. Hays,⁵³ C. Hebert,⁴⁴ D. Hedin,³⁹ J.M. Heinmiller,³⁸ A.P. Heinson,³⁴
 U. Heintz,⁴⁸ T. Heuring,³⁵ M.D. Hildreth,⁴² R. Hirosky,⁶³ J.D. Hobbs,⁵⁵ B. Hoeneisen,⁸
 Y. Huang,⁵⁰ R. Illingworth,²⁸ A.S. Ito,³⁷ M. Jaffré,¹¹ S. Jain,¹⁷ R. Jesik,²⁸ K. Johns,²⁹
 M. Johnson,³⁷ A. Jonckheere,³⁷ M. Jones,³⁶ H. Jöstlein,³⁷ A. Juste,³⁷ W. Kahl,⁴⁵ S. Kahn,⁵⁶
 E. Kajfasz,¹⁰ A.M. Kalinin,²³ D. Karmanov,²⁵ D. Karmgard,⁴² Z. Ke,⁴ R. Kehoe,⁵¹ A. Khanov,⁴⁵
 A. Kharchilava,⁴² S.K. Kim,¹⁸ B. Klima,³⁷ B. Knuteson,³⁰ W. Ko,³¹ J.M. Kohli,¹⁵
 A.V. Kostritskiy,²⁶ J. Kotcher,⁵⁶ B. Kothari,⁵³ A.V. Kotwal,⁵³ A.V. Kozelov,²⁶ E.A. Kozlovsky,²⁶
 J. Krane,⁴³ M.R. Krishnaswamy,¹⁷ P. Krivkova,⁶ S. Krzywdzinski,³⁷ M. Kubantsev,⁴⁵
 S. Kuleshov,²⁴ Y. Kulik,⁵⁵ S. Kunori,⁴⁷ A. Kupco,⁷ V.E. Kuznetsov,³⁴ G. Landsberg,⁵⁹
 W.M. Lee,³⁵ A. Leflat,²⁵ C. Leggett,³⁰ F. Lehner,^{37,*} J. Li,⁶⁰ Q.Z. Li,³⁷ X. Li,⁴ J.G.R. Lima,³
 D. Lincoln,³⁷ S.L. Linn,³⁵ J. Linnemann,⁵¹ R. Lipton,³⁷ A. Lucotte,⁹ L. Lueking,³⁷
 C. Lundstedt,⁵² C. Luo,⁴¹ A.K.A. Maciel,³⁹ R.J. Madaras,³⁰ V.L. Malyshev,²³ V. Manankov,²⁵
 H.S. Mao,⁴ T. Marshall,⁴¹ M.I. Martin,³⁹ R.D. Martin,³⁸ K.M. Mauritz,⁴³ B. May,⁴⁰
 A.A. Mayorov,⁴¹ R. McCarthy,⁵⁵ T. McMahan,⁵⁷ H.L. Melanson,³⁷ M. Merkin,²⁵ K.W. Merritt,³⁷
 C. Miao,⁵⁹ H. Miettinen,⁶² D. Mihalcea,³⁹ C.S. Mishra,³⁷ N. Mokhov,³⁷ N.K. Mondal,¹⁷
 H.E. Montgomery,³⁷ R.W. Moore,⁵¹ M. Mostafa,¹ H. da Motta,² E. Nagy,¹⁰ F. Nang,²⁹
 M. Narain,⁴⁸ V.S. Narasimham,¹⁷ H.A. Neal,⁵⁰ J.P. Negret,⁵ S. Negroni,¹⁰ T. Nunnemann,³⁷
 D. O'Neil,⁵¹ V. Oguri,³ B. Olivier,¹² N. Oshima,³⁷ P. Padley,⁶² L.J. Pan,⁴⁰ K. Papageorgiou,³⁸
 A. Para,³⁷ N. Parashar,⁴⁹ R. Partridge,⁵⁹ N. Parua,⁵⁵ M. Paterno,⁵⁴ A. Patwa,⁵⁵ B. Pawlik,²²

J. Perkins,⁶⁰ M. Peters,³⁶ O. Peters,²⁰ P. Pétrouff,¹¹ R. Piegaia,¹ B.G. Pope,⁵¹ E. Popkov,⁴⁸ H.B. Prosper,³⁵ S. Protopopescu,⁵⁶ J. Qian,⁵⁰ R. Raja,³⁷ S. Rajagopalan,⁵⁶ E. Ramberg,³⁷ P.A. Rapidis,³⁷ N.W. Reay,⁴⁵ S. Reucroft,⁴⁹ M. Ridel,¹¹ M. Rijssenbeek,⁵⁵ F. Rizatdinova,⁴⁵ T. Rockwell,⁵¹ M. Roco,³⁷ P. Rubinov,³⁷ R. Ruchti,⁴² J. Rutherford,²⁹ B.M. Sabirov,²³ G. Sajot,⁹ A. Santoro,² L. Sawyer,⁴⁶ R.D. Schamberger,⁵⁵ H. Schellman,⁴⁰ A. Schwartzman,¹ N. Sen,⁶² E. Shabalina,³⁸ R.K. Shivpuri,¹⁶ D. Shpakov,⁴⁹ M. Shupe,²⁹ R.A. Sidwell,⁴⁵ V. Simak,⁷ H. Singh,³⁴ J.B. Singh,¹⁵ V. Sirotenko,³⁷ P. Slattery,⁵⁴ E. Smith,⁵⁸ R.P. Smith,³⁷ R. Snihur,⁴⁰ G.R. Snow,⁵² J. Snow,⁵⁷ S. Snyder,⁵⁶ J. Solomon,³⁸ V. Sorín,¹ M. Sosebee,⁶⁰ N. Sotnikova,²⁵ K. Soustruznik,⁶ M. Souza,² N.R. Stanton,⁴⁵ G. Steinbrück,⁵³ R.W. Stephens,⁶⁰ F. Stichelbaut,⁵⁶ D. Stoker,³³ V. Stolin,²⁴ A. Stone,⁴⁶ D.A. Stoyanova,²⁶ M. Strauss,⁵⁸ M. Strovink,³⁰ L. Stutte,³⁷ A. Sznajder,³ M. Talby,¹⁰ W. Taylor,⁵⁵ S. Tentindo-Repond,³⁵ S.M. Tripathi,³¹ T.G. Trippe,³⁰ A.S. Turcot,⁵⁶ P.M. Tuts,⁵³ P. van Gemmeren,³⁷ V. Vaniev,²⁶ R. Van Kooten,⁴¹ N. Varelas,³⁸ L.S. Vertogradov,²³ F. Villeneuve-Seguié,¹⁰ A.A. Volkov,²⁶ A.P. Vorobiev,²⁶ H.D. Wahl,³⁵ H. Wang,⁴⁰ Z.-M. Wang,⁵⁵ J. Warchol,⁴² G. Watts,⁶⁴ M. Wayne,⁴² H. Weerts,⁵¹ A. White,⁶⁰ J.T. White,⁶¹ D. Whiteson,³⁰ J.A. Wightman,⁴³ D.A. Wijngaarden,²¹ S. Willis,³⁹ S.J. Wimpenny,³⁴ J. Womersley,³⁷ D.R. Wood,⁴⁹ R. Yamada,³⁷ P. Yamin,⁵⁶ T. Yasuda,³⁷ Y.A. Yatsunenko,²³ K. Yip,⁵⁶ S. Youssef,³⁵ J. Yu,³⁷ Z. Yu,⁴⁰ M. Zanabria,⁵ H. Zheng,⁴² Z. Zhou,⁴³ M. Zielinski,⁵⁴ D. Zieminska,⁴¹ A. Ziemiński,⁴¹ V. Zutshi,⁵⁶ E.G. Zverev,²⁵ and A. Zylberstejn¹³

(DØ Collaboration)

¹Universidad de Buenos Aires, Buenos Aires, Argentina

²LAFEX, Centro Brasileiro de Pesquisas Físicas, Rio de Janeiro, Brazil

³Universidade do Estado do Rio de Janeiro, Rio de Janeiro, Brazil

⁴Institute of High Energy Physics, Beijing, People's Republic of China

⁵Universidad de los Andes, Bogotá, Colombia

⁶Charles University, Center for Particle Physics, Prague, Czech Republic

⁷Institute of Physics, Academy of Sciences, Center for Particle Physics, Prague, Czech Republic

⁸Universidad San Francisco de Quito, Quito, Ecuador

⁹Institut des Sciences Nucléaires, IN2P3-CNRS, Université de Grenoble 1, Grenoble, France

¹⁰CPPM, IN2P3-CNRS, Université de la Méditerranée, Marseille, France

¹¹Laboratoire de l'Accélérateur Linéaire, IN2P3-CNRS, Orsay, France

¹²LPNHE, Universités Paris VI and VII, IN2P3-CNRS, Paris, France

¹³DAPNIA/Service de Physique des Particules, CEA, Saclay, France

¹⁴Universität Mainz, Institut für Physik, Mainz, Germany

¹⁵Panjab University, Chandigarh, India

¹⁶Delhi University, Delhi, India

¹⁷Tata Institute of Fundamental Research, Mumbai, India

¹⁸Seoul National University, Seoul, Korea

¹⁹CINVESTAV, Mexico City, Mexico

²⁰FOM-Institute NIKHEF and University of Amsterdam/NIKHEF, Amsterdam, The Netherlands

²¹University of Nijmegen/NIKHEF, Nijmegen, The Netherlands

²²Institute of Nuclear Physics, Kraków, Poland

²³Joint Institute for Nuclear Research, Dubna, Russia

²⁴Institute for Theoretical and Experimental Physics, Moscow, Russia

- ²⁵Moscow State University, Moscow, Russia
- ²⁶Institute for High Energy Physics, Protvino, Russia
- ²⁷Lancaster University, Lancaster, United Kingdom
- ²⁸Imperial College, London, United Kingdom
- ²⁹University of Arizona, Tucson, Arizona 85721
- ³⁰Lawrence Berkeley National Laboratory and University of California, Berkeley, California 94720
- ³¹University of California, Davis, California 95616
- ³²California State University, Fresno, California 93740
- ³³University of California, Irvine, California 92697
- ³⁴University of California, Riverside, California 92521
- ³⁵Florida State University, Tallahassee, Florida 32306
- ³⁶University of Hawaii, Honolulu, Hawaii 96822
- ³⁷Fermi National Accelerator Laboratory, Batavia, Illinois 60510
- ³⁸University of Illinois at Chicago, Chicago, Illinois 60607
- ³⁹Northern Illinois University, DeKalb, Illinois 60115
- ⁴⁰Northwestern University, Evanston, Illinois 60208
- ⁴¹Indiana University, Bloomington, Indiana 47405
- ⁴²University of Notre Dame, Notre Dame, Indiana 46556
- ⁴³Iowa State University, Ames, Iowa 50011
- ⁴⁴University of Kansas, Lawrence, Kansas 66045
- ⁴⁵Kansas State University, Manhattan, Kansas 66506
- ⁴⁶Louisiana Tech University, Ruston, Louisiana 71272
- ⁴⁷University of Maryland, College Park, Maryland 20742
- ⁴⁸Boston University, Boston, Massachusetts 02215
- ⁴⁹Northeastern University, Boston, Massachusetts 02115
- ⁵⁰University of Michigan, Ann Arbor, Michigan 48109
- ⁵¹Michigan State University, East Lansing, Michigan 48824
- ⁵²University of Nebraska, Lincoln, Nebraska 68588
- ⁵³Columbia University, New York, New York 10027
- ⁵⁴University of Rochester, Rochester, New York 14627
- ⁵⁵State University of New York, Stony Brook, New York 11794
- ⁵⁶Brookhaven National Laboratory, Upton, New York 11973
- ⁵⁷Langston University, Langston, Oklahoma 73050
- ⁵⁸University of Oklahoma, Norman, Oklahoma 73019
- ⁵⁹Brown University, Providence, Rhode Island 02912
- ⁶⁰University of Texas, Arlington, Texas 76019
- ⁶¹Texas A&M University, College Station, Texas 77843
- ⁶²Rice University, Houston, Texas 77005
- ⁶³University of Virginia, Charlottesville, Virginia 22901
- ⁶⁴University of Washington, Seattle, Washington 98195
- * Visitor from University of Zurich, Zurich, Switzerland.

I. INTRODUCTION

Jet production in hadronic collisions is understood within the framework of Quantum Chromodynamics (QCD) as a hard scattering of constituent partons (quarks and gluons), which, having undergone the interaction, manifest themselves as showers of collimated particles called jets. Jet algorithms associate clusters of these particles into jets in a way that the kinematic properties of the hard-scattered partons can be inferred and thereby compared to predictions from perturbative QCD (pQCD).

Historically, only the cone algorithm has been used to reconstruct jets at hadron colliders [1]. Although well suited to implement the experimental corrections needed in the complex environment of hadron colliders, the cone algorithms used in previous measurements by the hadron collider experiments at the Fermilab Tevatron present several difficulties, because (a) an arbitrary procedure must be implemented to split and merge overlapping cones, (b) an ad-hoc parameter, \mathcal{R}_{sep} , is required to accommodate the differences between jet definitions at the parton and detector levels [2], and (c) improved theoretical predictions calculated at the Next-to-Next-to-Leading-Order (NNLO) in pQCD are not infrared safe, because they exhibit a marked sensitivity to soft radiation [3].

Inspired by QCD, a second class of jet algorithms, which does not suffer from these shortcomings, has been developed by several groups [4–6]. These clustering or recombination algorithms successively merge pairs of nearby vectors (partons, particles or calorimeter towers) in order of increasing relative transverse momentum (p_T). A single arbitrary parameter, D , which characterizes approximately the size of the resulting jets, is used to determine when this merging stops. No splitting-merging is involved, because each vector is assigned to a unique jet. There is no need for introducing any ad-hoc parameters, because the same algorithm is applied at the theoretical and experimental level. Furthermore, by design, clustering algorithms are infrared and collinear safe to all orders of calculation. The dependence of the inclusive jet cross section on the choice of reconstruction algorithms or parameters is particularly relevant for studying the effect of hadronization and background from spectator partons in the event. In contrast to previous work from hadron colliders [7–11], this paper presents the first measurement of the inclusive jet cross section using the k_{\perp} algorithm to reconstruct jets.

II. JET RECONSTRUCTION AND SELECTION

The differential jet cross section was measured in bins of p_T and pseudo-rapidity, $\eta \equiv -\ln[\tan(\theta/2)]$, where a right handed coordinate system is adopted with the z axis pointing in the proton beam direction, and θ is the polar angle. The k_{\perp} algorithm implemented at DØ [12] is based on the clustering algorithm suggested in Ref. [6]. The algorithm starts with a list of pre-clusters or “vectors”. For each vector $p_{T,i}$, $d_{ii} = p_{T,i}^2$, and for each pair of vectors, $d_{ij} = \min(p_{T,i}^2, p_{T,j}^2) \Delta R_{i,j}^2 / D^2$ are defined, where D is the free parameter of the algorithm and $\Delta R_{i,j}^2 = \Delta\phi_{ij}^2 + \Delta\eta_{ij}^2$ is the square of the angular separation between the vectors. If the minimum of all d_{ii} and d_{ij} is a d_{ij} , then the vectors i and j are merged, becoming the merged four-vector $(E_i + E_j, \vec{p}_i + \vec{p}_j)$. If the minimum is a d_{ii} , the vector i is defined as a jet.

This procedure is repeated until all vectors are combined into jets. Thus k_{\perp} jets do not have to include all vectors in a cone of radius D , and can include vectors outside of this cone.

The primary tool for jet detection at DØ is the uranium-liquid argon calorimeter [13], which has full coverage for pseudo-rapidity $|\eta| < 4.1$. The initial hardware trigger selected inelastic collisions as defined by hodoscopes located near the beam axis on both sides of the interaction region. The next stage required energy deposition in any $\Delta\eta \times \Delta\phi = 0.8 \times 1.6$ region of the calorimeter, corresponding to a transverse energy (E_T) above a preset threshold. Selected events were digitized and sent to an array of processors. Jet candidates were reconstructed with a cone algorithm (with radius $R = 0.7$), and the event was recorded if any jet E_T exceeded a specified threshold. Jet E_T thresholds of 30, 50, 85 and 115 GeV were used to accumulate integrated luminosities of 0.34, 4.46, 51.5 and 87.3 pb⁻¹, respectively [10].

Jets were reconstructed offline using the k_{\perp} algorithm, with $D = 1.0$. This value of D was chosen because, at next-to-leading-order (NLO), it produces a theoretical cross section that is essentially identical to the cone prediction for $R = 0.7$ [6], as used by DØ in its previous publications on jet production [10]. The imbalance in transverse momentum, “missing transverse energy”, was calculated from the vector sum of the E_T values in all cells of the calorimeter. The vertices of the events were reconstructed using the central tracking system [13]. A significant portion of the data was taken at high instantaneous luminosity, where more than one interaction per beam crossing was probable. When an event had more than one reconstructed vertex, the quantity $S_T = |\Sigma \vec{p}_T^{jet}|$ was defined for the two vertices that had the largest number of tracks, and the vertex with the smaller S_T was retained for calculating all kinematic variables. To preserve the pseudo-projective nature of the DØ calorimeter, the selected vertex was required to be within 50 cm of the center of the detector. This requirement rejected $(10.6 \pm 0.1)\%$ of the events, independent of jet transverse momentum.

Isolated noisy calorimeter cells were suppressed using online and offline algorithms [14]. Background introduced by electrons, photons, detector noise and accelerator losses that mimicked jets were eliminated with quality cuts. The efficiency of jet selection was approximately 99.5% and nearly independent of jet p_T . Background events from cosmic rays or misvertexed events were eliminated by requiring the missing transverse energy in each event to be less than 70% of the p_T of the leading jet. This criterion was nearly 100% efficient.

The DØ jet momentum calibration [12], applied on a jet by jet basis, corrects on average the reconstructed p_T for background from spectator partons (the “underlying event”, determined from minimum-bias events), additional interactions, pileup from previous $p\bar{p}$ crossings, noise from uranium radioactivity, detector non-uniformities, and for the global response of the detector to hadronic jets. Unlike the cone algorithm, the k_{\perp} algorithm does not require additional corrections for showering in the calorimeter [12]. For $|\eta| < 0.5$, the mean total multiplicative correction factor to an observed p_T of 100 GeV [400 GeV] was 1.094 ± 0.015 [1.067 ± 0.020].

III. INCLUSIVE CROSS SECTION

The inclusive jet cross section for $|\eta| < 0.5$ was calculated in four ranges of transverse momentum, using data from only one trigger in each case. The more restrictive trigger

was used as soon as it became fully efficient. The average differential cross section for each p_T bin, $d^2\sigma/(dp_T d\eta)$, was calculated as $N/(\Delta\eta\Delta p_T\epsilon\int Ldt)$, where $\Delta\eta$, Δp_T are the η , p_T bin sizes, N the number of jets observed in that bin, ϵ is the overall efficiency for jet and event selection, and $\int Ldt$ represents the integrated luminosity of the data sample.

The measured cross section is distorted in p_T by the momentum resolution of the DØ calorimeter. Although the resolution in jet p_T is essentially Gaussian, the steepness of the p_T spectrum shifts the observed cross section to larger values. The fractional momentum resolution was determined from the imbalance in p_T in two-jet events [14]. At 100 GeV [400 GeV] the fractional resolution was 0.061 ± 0.006 [0.039 ± 0.003]. The distortion in the cross section due to the resolution was corrected by assuming an ansatz function, $A p_T^{-B}(1 - 2p_T/\sqrt{s})^C$, smearing this with the measured resolution, and fitting the parameters A , B and C so as to best describe the observed cross section. The bin-to-bin ratio of the original ansatz to the smeared one was used to remove the distortion due to resolution. The unsmearing correction reduces the observed cross section by $(5.7 \pm 1)\%$ [$(6.1 \pm 1)\%$] at 100 GeV [400 GeV].

The final, fully corrected, cross section for $|\eta| < 0.5$ is shown in Fig. 1, along with statistical uncertainties. Listed in Table I are the p_T ranges, the point positions, the cross section, and uncertainties in each bin. The systematic uncertainties include contributions from jet and event selection, unsmearing, luminosity and the uncertainty in the momentum scale, which dominates at all transverse momenta. The fractional uncertainties for the different components are plotted in Fig. 2 as a function of the jet transverse momentum.

IV. COMPARISON WITH THEORY

The results are compared to the pQCD NLO prediction from JETRAD [15], with the renormalization and factorization scales set to $p_T^{max}/2$, where p_T^{max} refers to the p_T of the leading jet in an event. The comparisons are made using parametrizations of the parton distributions functions (PDFs) of the CTEQ [16] and MRST [17] families. Figure 3 shows the ratios of $(D - T)/T$, where D refers to data and T to the theoretical prediction. To quantify the comparison in Fig. 3, the fractional systematic uncertainties are multiplied by the predicted cross section and a χ^2 comparison is carried out. The results are shown in Table II. The agreement is reasonable (χ^2/dof ranges from 1.56 to 1.12, the probabilities from 4 to 31%), although the differences in normalization and shape, especially at low p_T , are quite large. The points at low p_T have the highest impact on the χ^2 . If the first four data points are not used in the χ^2 comparison, the probabilities increase to the 60 – 80% range.

V. CONCLUSIONS

In conclusion, a preliminary measurement in proton-antiproton collisions at $\sqrt{s} = 1.8$ TeV of the inclusive jet cross section based on the k_\perp algorithm has been presented. The quantitative test shows reasonable agreement between data and NLO pQCD predictions.

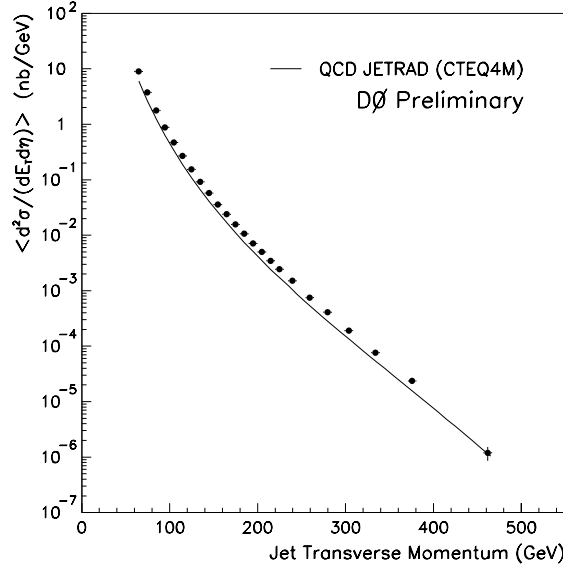


FIG. 1. The central ($|\eta| < 0.5$) inclusive jet cross section obtained with the k_{\perp} algorithm at $\sqrt{s} = 1.8$ TeV. Only statistical errors are included. The solid line shows a prediction from NLO pQCD.

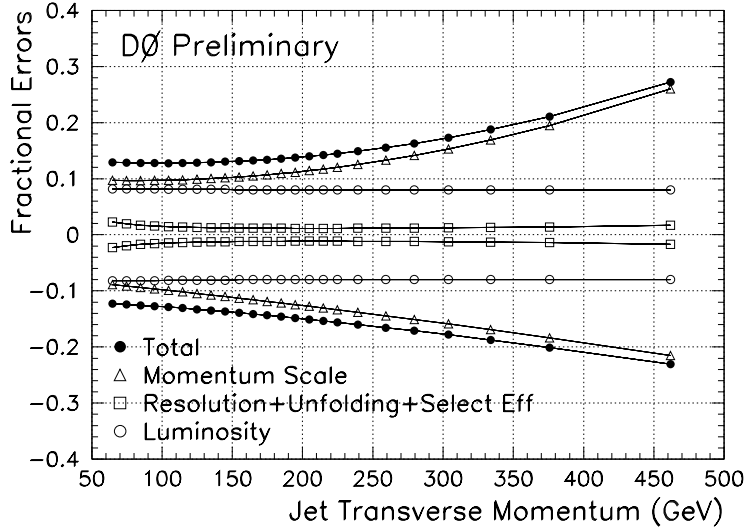


FIG. 2. Fractional experimental uncertainties on the cross section.

| Bin Range (GeV) | Plotted p_T (GeV) | Cross Sec. \pm Stat. (nb/GeV) | Systematic Uncer (%) |
|--------------------|------------------------|------------------------------------|-------------------------|
| 60 – 70 | 64.6 | $(8.94 \pm 0.06) \times 10^0$ | -13, +14 |
| 70 – 80 | 74.6 | $(3.78 \pm 0.04) \times 10^0$ | -13, +14 |
| 80 – 90 | 84.7 | $(1.77 \pm 0.02) \times 10^0$ | -13, +14 |
| 90 – 100 | 94.7 | $(8.86 \pm 0.25) \times 10^{-1}$ | -13, +14 |
| 100 – 110 | 104.7 | $(4.68 \pm 0.04) \times 10^{-1}$ | -14, +14 |
| 110 – 120 | 114.7 | $(2.68 \pm 0.03) \times 10^{-1}$ | -14, +14 |
| 120 – 130 | 124.8 | $(1.53 \pm 0.02) \times 10^{-1}$ | -14, +14 |
| 130 – 140 | 134.8 | $(9.19 \pm 0.16) \times 10^{-2}$ | -14, +14 |
| 140 – 150 | 144.8 | $(5.77 \pm 0.12) \times 10^{-2}$ | -14, +14 |
| 150 – 160 | 154.8 | $(3.57 \pm 0.03) \times 10^{-2}$ | -15, +14 |
| 160 – 170 | 164.8 | $(2.39 \pm 0.02) \times 10^{-2}$ | -15, +14 |
| 170 – 180 | 174.8 | $(1.56 \pm 0.02) \times 10^{-2}$ | -15, +14 |
| 180 – 190 | 184.8 | $(1.05 \pm 0.02) \times 10^{-2}$ | -15, +14 |
| 190 – 200 | 194.8 | $(7.14 \pm 0.13) \times 10^{-3}$ | -16, +15 |
| 200 – 210 | 204.8 | $(4.99 \pm 0.08) \times 10^{-3}$ | -16, +15 |
| 210 – 220 | 214.8 | $(3.45 \pm 0.07) \times 10^{-3}$ | -16, +15 |
| 220 – 230 | 224.8 | $(2.43 \pm 0.06) \times 10^{-3}$ | -16, +15 |
| 230 – 250 | 239.4 | $(1.50 \pm 0.03) \times 10^{-3}$ | -17, +16 |
| 250 – 270 | 259.4 | $(7.52 \pm 0.23) \times 10^{-4}$ | -17, +16 |
| 270 – 290 | 279.5 | $(4.07 \pm 0.17) \times 10^{-4}$ | -18, +17 |
| 290 – 320 | 303.8 | $(1.93 \pm 0.09) \times 10^{-4}$ | -18, +18 |
| 320 – 350 | 333.9 | $(7.61 \pm 0.59) \times 10^{-5}$ | -19, +19 |
| 350 – 410 | 375.8 | $(2.36 \pm 0.23) \times 10^{-5}$ | -20, +21 |
| 410 – 560 | 461.8 | $(1.18 \pm 0.33) \times 10^{-6}$ | -23, +27 |

TABLE I. Single inclusive cross section with jets reconstructed using the k_{\perp} algorithm in the central pseudo-rapidity region.

| PDF | χ^2 | χ^2/dof | Probability (%) |
|--------------------|----------|--------------|-----------------|
| MRST | 26.8 | 1.12 | 31 |
| MRSTg \uparrow | 33.1 | 1.38 | 10 |
| MRSTg \downarrow | 28.2 | 1.17 | 25 |
| CTEQ3M | 37.5 | 1.56 | 4 |
| CTEQ4M | 31.2 | 1.30 | 15 |
| CTEQ4HJ | 27.2 | 1.13 | 29 |

TABLE II. χ^2 comparisons (24 degrees of freedom) between JETRAD, with renormalization and factorization scales set to $p_T^{max}/2$, and data for various PDFs.

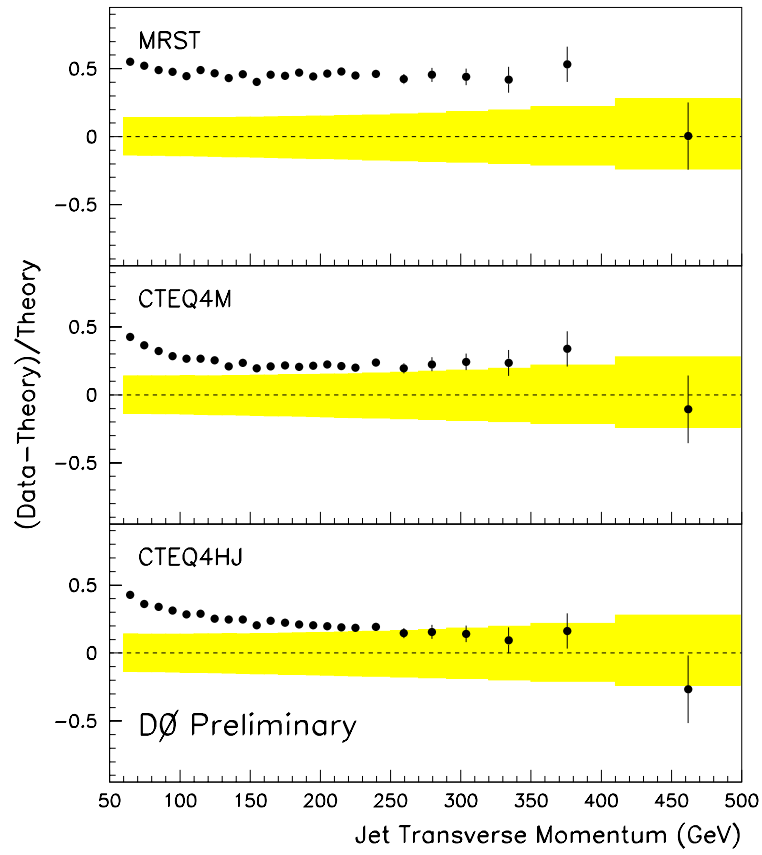


FIG. 3. Difference between data and JETRAD pQCD normalized to predictions. The outer error bars represent the total systematic uncertainty.

ACKNOWLEDGEMENTS

We thank the staffs at Fermilab and collaborating institutions, and acknowledge support from the Department of Energy and National Science Foundation (USA), Commissariat à L'Energie Atomique and CNRS/Institut National de Physique Nucléaire et de Physique des Particules (France), Ministry for Science and Technology and Ministry for Atomic Energy (Russia), CAPES and CNPq (Brazil), Departments of Atomic Energy and Science and Education (India), Colciencias (Colombia), CONACyT (Mexico), Ministry of Education and KOSEF (Korea), CONICET and UBACyT (Argentina), The Foundation for Fundamental Research on Matter (The Netherlands), PPARC (United Kingdom), Ministry of Education (Czech Republic), and the A.P. Sloan Foundation.

REFERENCES

- [1] J. Huth *et al.*, in proceedings of *Research Directions for the Decade, Snowmass 1990*, edited by E.L. Berger (World Scientific, Singapore, 1992).
- [2] B. Abbott *et al.* (DØ Coll.), FERMILAB-Pub-97/2442-E (1997).
- [3] W.T. Giele and W.B. Kilgore, Phys. Rev. D **55** 7183 (1997).
- [4] S. Catani, Yu.L. Dokshitzer, M.H. Seymour, and B.R. Webber, Nucl. Phys. B **406** 187 (1993).
- [5] S. Catani, Yu.L. Dokshitzer, and B.R. Webber, Phys. Lett. B **285** 291 (1992).
- [6] S.D. Ellis and D.E. Soper, Phys. Rev. D **48** 3160 (1993).
- [7] F. Abe *et al.*, (CDF Coll.), Phys. Rev. Lett. **77** 438 (1996).
- [8] B. Abbott *et al.* (DØ Coll.), Phys. Rev. Lett. **82** 2451 (1999).
- [9] B. Abbott *et al.* (DØ Coll.), Phys. Rev. Lett. **86** 1707 (2001)
- [10] B. Abbott *et al.* (DØ Coll.), hep-ex/0012046 submitted to Phys. Rev. D.
- [11] T. Affolder *et al.*, (CDF Coll.), submitted to Phys. Rev. D, January 18, 2001.
- [12] W.T. Giele *et al.* (Jet Physics Working Group), in Proceedings of the Fermilab Run II Workshop on QCD and Weak Boson Physics (2000) (to be published).
- [13] S. Abachi *et al.* (DØ Coll.), Nucl. Instr. Meth. Phys. Res. A **338**, 185 (1994).
- [14] S. Grinstein, Ph.D. thesis, Univ. de Buenos Aires, Argentina, 2001 (in preparation).
- [15] W.T. Giele, E.W.N. Glover, and D.A. Kosower, Phys. Rev. Lett. **73** , 2019 (1994).
- [16] H.L. Lai *et al.*, Phys. Rev. D **55**, 1280 (1997).
- [17] A. D. Martin *et al.*, Eur. Phys. J. C **4**, 463 (1998).